REACTION TRAJECTORIES IN THE HADRONIC PHASE TRANSITION REGION

David H. Boal[†]
Department of Physics
University of Illinois at Urbana-Champaign
1110 West Green Street
Urbana, IL 61801

ABSTRACT

Computer simulations are used to find the trajectories of nuclear reactions in the liquid-gas and quark-hadron phase transition regimes. It is found that proton induced and heavy ion induced reactions at intermediate energies enter the liquid-gas transition region, albeit in different ways. The simulations also show that the quark-hadron phase transition region should be accessable in heavy ion reactions at $\sqrt{s_{NN}} > 40$ GeV/c.

1. INTRODUCTION

One of the problems in accelerator based searches for signatures of hadronic phase transitions[*] is that the reactions are, by their very nature, time dependent: any possible phase transition (using the word loosely here) is a transient phenomenon whose effects may be obscured by the subsequent evolution of the reaction. One method of dealing with the time evolution of such finite systems is the use of computer simulations. Subject to the accuracy of the model, simulations may allow one to find out whether a particular reaction

---

[†]Permanent address: Dept. of Physics, Simon Fraser University, Burnaby, B.C. V5A 1S6 Canada.

*Since this is not meant to be a review paper, the interested reader is referred to the many other articles in this proceedings for further references. The references quoted in this paper are only those which pertain directly to the text.

accesses the phase transition region, what experimentally observable effects are generated by the transition and whether any of these effects survive the further evolution of the system. The finite size of the reaction region is obviously included as well. In this paper, some aspects of the nuclear liquid-gas transition will be investigated via computer simulation for both proton and heavy ion induced reactions. As well, ultra-relativistic heavy ion collisions will be examined to see if the conditions appropriate to the formation of a quark-gluon plasma can be achieved.

2. LIQUID-GAS TRANSITION.

2.1 Phase Diagram

Many calculations have been performed in the past decade or more delineating the liquid-gas coexistence regions of nuclear matter. One example[1] which used a zero range Skyrme interaction, is shown in Fig. 1. Curves of constant entropy per nucleon (S/A) are indicated by the dashed lines. The unstable regions are bounded by the

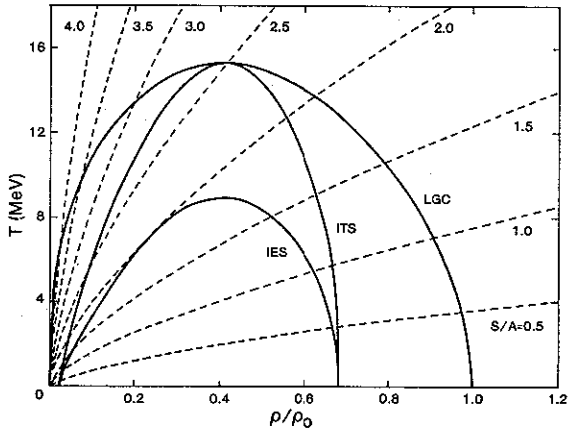

Figure 1. Phase diagram for nuclear matter from zero range Skyrme interaction of Ref. 1. The dashed curves are isentropes with the value of S/A indicated for each. Shown as well are the liquid-gas coexistence boundary (LGC), isothermal spinodal (ITS) and isentropic spinodal (IES).

isothermal spinodal (ITS) and isentropic spinodal (IES) curves. It is clear from the analysis of low and intermediate energy nuclear reaction data (for example, the two particle correlation measurements described elsewhere in these proceedings) that the trajectories of these reactions traverse the phase transition region near freeze out: typical temperatures at freeze-out are a few MeV and densities are of the order $1/2\ \rho_o$. Although the current data analysis methods are mainly concerned with the freeze-out region, the information they yield can be used as a check on the simulations. For example, in Ref. 2 the NN scattering rate was compared with the rate of expansion of an isotropic fireball to estimate its freeze-out characteristics. Such comparisons with data give one at least some confidence that the results of the simulations can be trusted for other parts of the reaction trajectory.

2.2 Proton - Induced Reactions

Proton (and presumably electron) induced reactions have the advantage of producing a system whose density is relatively uniform compared to the large scale inhomogeneities which may be present in a heavy ion reaction. Their disadvantage, for both experiments and simulations, is the low yield of fragment products. Hence, most of the discussion of fragmentation will be deferred to the following section on heavy ion reactions for the sake of providing better statistics. However, there are some simplifications which, while they would be unjustified for heavy ion reactions, are not too bad for the initial stages of a proton induced reaction. These simplifications allow a tremendous decrease in computer execution time per event and, in turn, allow calculation of some quantities which require good statistics. The model is as follows:

The simulation is performed for a single nucleon on a one hundred nucleon target. The motion of the particles is followed classically. The target nucleons are placed in a space-fixed square well potential (it can be verified by using the mean field generated potential model described in 2.3 that this is not a bad approximation

in proton induced reactions as long as the reaction time frame is kept short, less than 60 fm/c). The Pauli principle is incorporated only crudely:

i) The momenta of the nucleons in the target obey a Fermi distribution.

ii) A NN collision is considered Pauli blocked unless the final momenta of both nucleons are lifted above the Fermi surface.

Further details can be found in Ref. 1. There are two results from this calculation which will be commented on. The first is the distribution of unbound nucleons in momentum space. Shown in Fig. 2 is the distribution 24 fm/c after the projectile nucleon has entered the target. One can see the semi-circular contours of constant probability characteristic of the thermal model analysis[3] of the (p,p') data show through clearly. The absolute normalization of the distribution is also in the right range. However, even though this distribution is similar to what one expects from a single equilibrated reaction region, in fact, the system is only barely in equilibrium. (In other words, the coordinate space density, and hence the collision rate which maintains equilibrium, is very low).

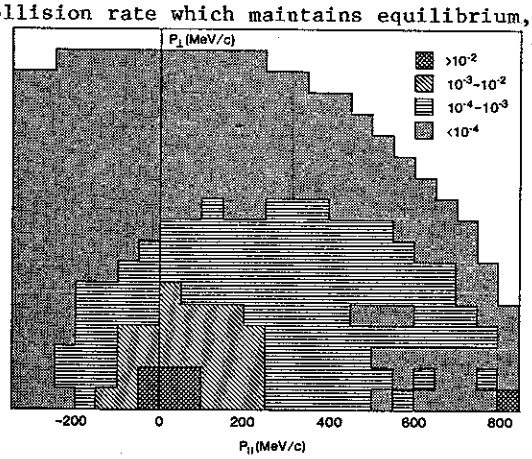

Figure 2. Model prediction for the free particle momentum space density in an impact parameter averaged 300 MeV p + (N = Z = 50) collision. The density is given in units of nucleons per $(50\ \mathrm{MeV/c})^3$. Nucleons bound in the nucleus are not included in this plot. The distribution was sampled at 8×10^{-23} sec after the projectile has entered the nucleus. From Ref. 1.

However, what is relevant for the phase transition is the reaction trajectory. It has been proposed[4] that fragment formation in proton induced reactions at much higher energies than those considered here, may proceed via condensation near the critical point. Since pion production is not included in the simple model under consideration here, we have nothing to say about such high energy fragmentation. What we can say at lower energies based on the free nucleon multiplicity, is that events with enough nucleons emitted to form a sizeable fragment are very rare. It is more likely that fragmentation in this regime corresponds to breakup of the residual system. To find out if the system actually reaches the mechanical instability region, the numerically generated energy occupation probability f(ε) is integrated directly to give the entropy:

$$S = -\int_0^\infty d\varepsilon\, D(\varepsilon)\,\left[f(\varepsilon)\,\ln f(\varepsilon) + \{1 - f(\varepsilon)\}\ln\{1 - f(\varepsilon)\}\right] \qquad (1)$$

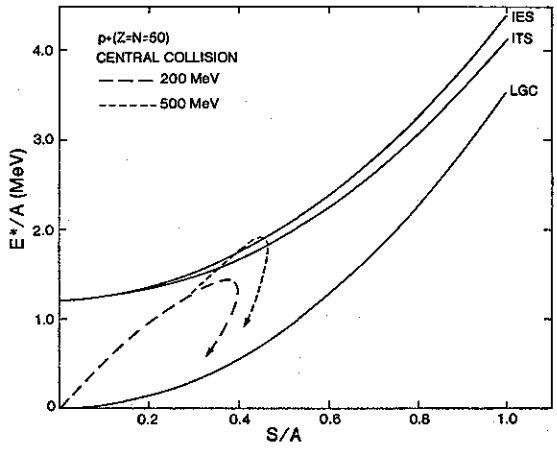

Figure 3. Isothermal spinodal (ITS), isentropic spinodal (IES) and liquid-gas coexistence curve (LGC) shown as a function of excitation energy and entropy per nucleon. The reaction trajectories for the excited nuclear system predicted by the model for 200 and 500 MeV p + (N = Z = 50) central collisions are shown by the dashed lines. From Ref. 1.

where $D(\varepsilon)$ is the density of states. The results of the calculation are illustrated in Fig. 3, where the reaction trajectory is shown as a function of E^*/A (excitation energy per nucleon) and S/A for a central collision at two bombarding energies. (What is shown is the entropy of the nucleons within the target radius, not the entropy of the system as a whole). One can see that the trajectory does reach the isentropic spinodal. One can assume a chemical equilibrium model at breakup to predict the fragment yields, with the parameters of the model being determined by where the trajectory intersects the isentropic spinodal. While the predicted yields are in at least qualitative agreement with the data, this does not constitute proof of spinodal decomposition.

2.3 Heavy Ion Reactions

The fixed target potential simplification which we used above for proton induced reactions is clearly inapplicable for heavy ion reactions and one must find a better way of handling the nucleus. One such approach, which has been used[5] in simulations of the Boltzmann equation, is to introduce a density dependent mean field $U(\rho)$ which allows the nucleons to bind together and form a nucleus. In the Boltzmann simulations, the density is an averaged quantity. Gale and Das Gupta[6] suggested that one could also use the mean field to propagate the fluctuations generated in an individual collision event. The model[7,8] which we wish to use here to investigate the phase transition region uses both a mean field and scattering terms, and, as such, is related to the Vlasov-Uehling-Uhlenbeck equation (VUU). However, the model is still essentially a classical equation of motion calculation, as can be seen from its ingredients:

i) Subject to certain constraints, a random initialization is made for the positions and momenta of the nucleons in a nucleus.

ii) The nucleon's position in phase space is smeared by means of a Gaussian of the form $\exp\{-[\alpha^2(\Delta r)^2] - [(\Delta p)^2/(\hbar\alpha)^2]\}$.

The smeared positions are used to calculate densities in both phase space and coordinate space.

iii) The coordinate space positions of the nucleons are propagated classically according to the variation in $U(\rho)$.

iv) A collision term is present, and the phase space occupancy is used to determine whether a given collision is allowed.

The only place where a quantum mechanical effect comes in (aside from the initial Fermi gas momentum distribution which is put in by hand) is in the Pauli blocking present in the collision term. For example, there is no variable de Broglie wavelength associated with each particle, and the only way that identical particles can be kept out of each other's phase space is through the collision term. Nevertheless, we feel that it is a useful first step on the way to constructing a quantum mechanical model.

Only a few of the results we have compiled will be touched on. For brevity, we will restrict ourselves to results for an equal mass collision of two ($Z = N = 20$) nuclei at 150 A•MeV in the lab. A scatter plot of the products of the reaction as a function of impact parameter (b) is shown in Fig. 4. As one would expect, collisions at large impact parameter do very little damage to the original nuclei: the greatest proportion of fragments come from more central collisions. Let's specialize to central collisions, then, and follow their temporal evolution.

One calculation which was performed was to follow the local coordinate and phase space density observed by nucleons which ultimately emerged as members of a cluster of given mass. The average coordinate space density is shown in Fig. 5 for several cluster masses: 1, 4 and 30. One can see that the average local density for each of the clusters starts out at about the same value at 20 fm/c, corresponding to maximum overlap of the target and projectile. The mass 1 systems observe a local density which simply decreases with time, as the free nucleons become further separated from nearby clusters. The mass 30 systems show very different behavior, which we observed for all heavy systems. The average

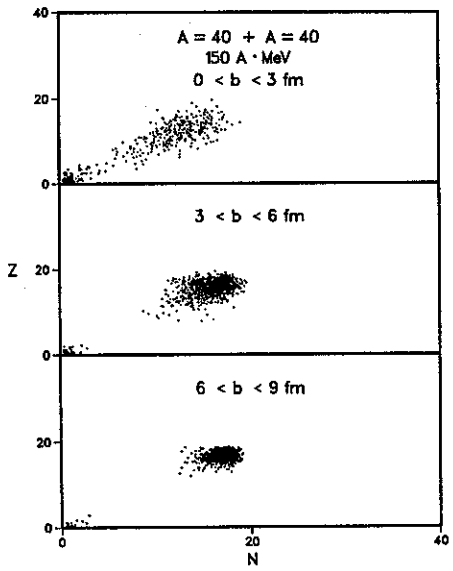

Figure 4. Scatter plots for the reaction products predicted by the VUU model for equal mass (Z = N = 20) collisions at 150 A•MeV. Three ranges of impact parameter are shown: 0-3 fm, 3-6 fm and 6-9 fm. From Ref. 7.

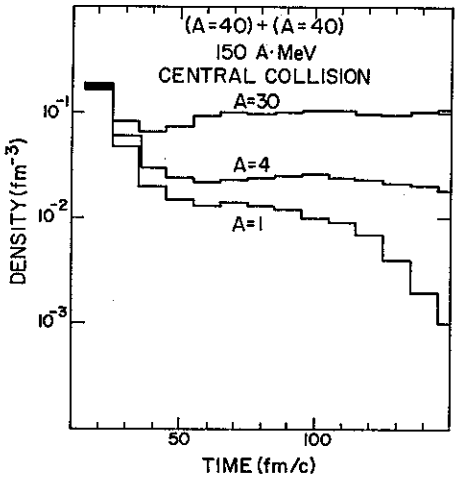

Figure 5. Average coordinate space density for several cluster masses (A = 1, 4, 30) shown as a function of time for a central collision of two (A = 40) nuclei at 150 A•MeV in the VUU model. From Ref. 7.

spatial density decreases, usually to about 0.06 fm^{-3}, then increases and oscillates about its asymptotic value (the average density of a light nucleus will be considerably less than the central value). This behavior is what one expects from the mechanical instability region: if a system has enough energy to enter the region at low density, it fragments; if it does not have enough energy, it oscillates. This effect can be seen even more dramatically in Fig. 6, where the average phase space density is shown for the same cluster masses. Even at t = 20 fm/c, where the coordinate space densities for all the clusters are similar, the phase space densities are very different. Nucleons which emerge as free particles already have been scattered into low density regions of phase space at this early stage of the reaction. The nucleons of heavy systems remain in relatively constant density regions throughout.

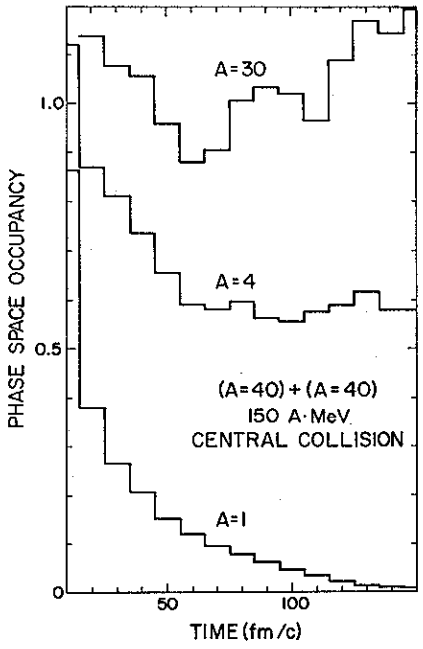

Figure 6. Average phase space occupancy for the same conditions as Fig. 5. From Ref. 7.

In summary, a picture of fragmentation at intermediate energy emerges in which the phase space fluctuations are the driving force behind the eventual outcome of a reaction. However, we have not yet found a way of inverting experimentally measured yields to determine where the instability boundary lies.

3. ULTRA-RELATIVISTIC HEAVY ION COLLISIONS

We now wish to shift our energy scale abruptly and work in the language of quarks and gluons. In this paper, we will limit ourselves to looking at the question of thermalization in an ultra-relativistic heavy ion collision. The method we adopt to look at this question is the parton cascade model,[9] which is certainly not applicable in the non-perturbative regime, but may be approximately valid for predicting certain quantities in the perturbative regime. A brief outline of the model's ingredients is:

i) Nucleons are represented by 3 quarks and 5 gluons each, the fractional momentum x carried by each massless parton being randomly assigned according to the distributions found from deep inelastic scattering.[10]

ii) The trajectories of the partons are followed classically and the parton collision cross sections are taken from lowest order QCD.[11].

iii) In a collision, the partons may be scattered off mass shell according to a m^{-2} distribution. They decay with a lifetime of $\hbar/\alpha_s m$. The decay products are two collinear massless partons with momentum fraction distributed according to the Altarelli-Parisi[12] splitting functions.

There are no antiquarks present in the initialization chosen; in this model they are produced only through collisions. Hence, the time evolution of their energy density provides a simple means of following the thermalization step of the collision. For example, in a central (A = 50) + (A = 50) collision at $\sqrt{s_{NN}}$ = 40 GeV the antiquark energy density reaches a maximum at 4×10^{-24} sec after the nuclei begins to interpenetrate. Similar results were found for

other reactions. Thus, a time scale of $\sim 1/2 \times 10^{-23}$ sec seems to be indicated for the thermalization step.

To see whether the gluons, which carry much of the momentum, are reasonably thermalized, we show their distribution in momentum space in Fig. 7. The reaction is (A = 50) + (A = 50) at $\sqrt{s_{NN}}$ = 40 GeV with the reaction stopped at 6×10^{-24} sec. The top part of Fig. 7 shows the distribution of all of the gluons (an average of 1500 per event;

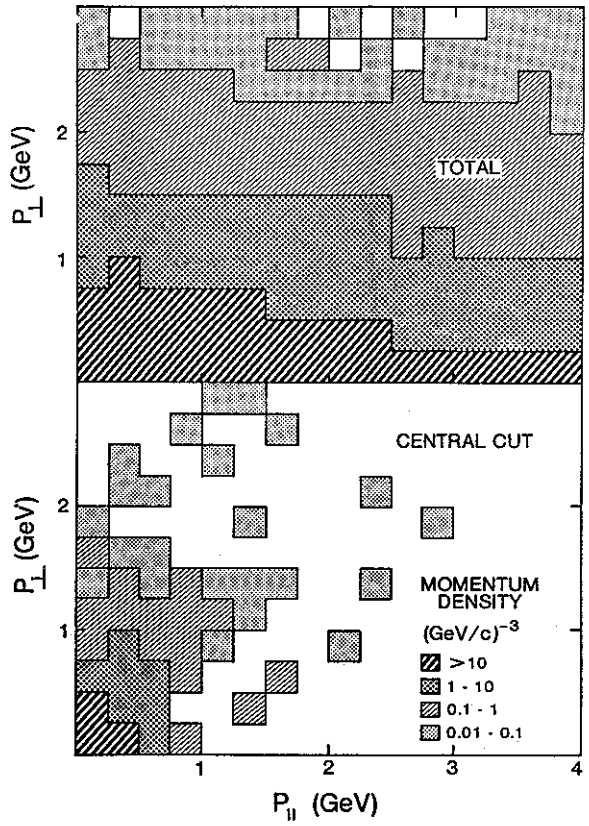

Figure 7. Momentum distribution of gluons in a central (A = 50) + (A = 50) collision at $\sqrt{s_{NN}}$ = 40 GeV observed at 6×10^{-24} sec after the nuclei begin to overlap. Distributions for all the gluons, and for those subject to a central cut in coordinate space, are shown. From Ref. 9.

40 events were summed over) in the directions perpendicular and parallel to the collision axis. One can see that there is a strong longitudinal component to the distribution. However, if one makes a central cut in coordinate space, the distribution is much more isotropic. The cut used in the lower part of Fig. 7 is a cylinder 2 fm in length and 1 fm in radius centered on the center of mass. Enlarging the coordinate space cut in the perpendicular direction introduces more of a perpendicular component to the distribution, corresponding to radial flow.

Having established that the central region is fairly thermalized, the major question is what is the energy density. For the reaction shown in Fig. 7, the energy density associated with the

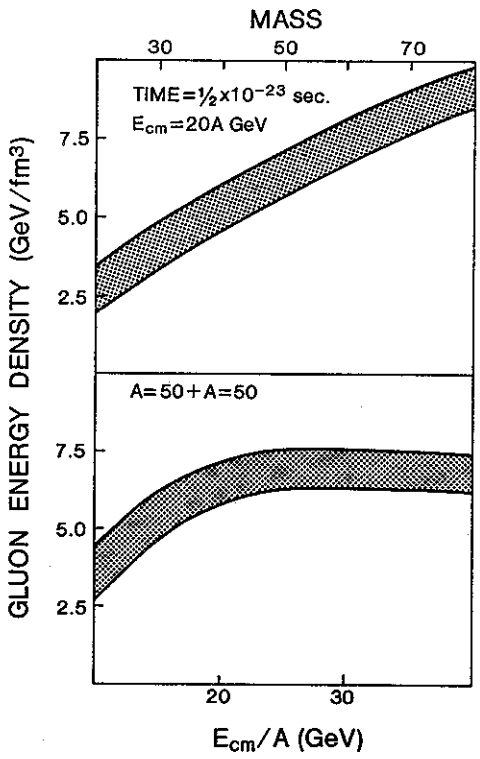

Figure 8. Mass and bombarding energy dependence of the gluon energy density in the central region from Ref. 9.

gluons in the central region is 5 GeV/fm^3. In this code, chemical equilibrium has not been established among the species by 5×10^{-24} sec, and most of the energy is carried by the gluons. However, this value is still more than the few GeV/fm^3 which, it is argued, is required for plasma formation. Larger energy densities can be achieved by increasing either the energy or mass. Examples are shown in Fig. 8 for the gluon energy density in a central region defined as a cylinder 1 fm in length, 3 fm in radius with the reaction stopped at 5×10^{-24} sec. The top part of the figure illustrates the mass dependence (equal projectile and target masses) for a (20 A•GeV) + (20 A•GeV) central collision. Calculations were carried out to (A = 100) + (A = 100), beyond which execution time became prohibitively long (3 CPU hours/event at 5 mips). The cross-hatched region represents the uncertainty caused by using only a finite number of events. By using large nuclei, energy densities in excess of 10 GeV/fm^3 can be achieved. In the calculations performed so far, the dependence of the energy density on bombarding energy is not so pronounced. For an (A = 50) + (A = 50) collision, the energy density appears to flatten out above 20 A•GeV in the center of mass, as shown in the lower portion of Fig. 8.

To summarize, using the parton cascade approach, we have demonstrated that the central region in coordinate space achieves approximate thermalization after $1/2 \times 10^{-23}$ sec in an ultra-relativistic collision. The region is baryon number depleted, particularly when comparing the net baryon number density with the gluon number density. The energy densities achievable appear to be quite adequate for the formation of the quark-gluon plasma state, particularly for projectile/target masses in excess of 100 and center of mass energies above $\sqrt{s_{NN}} = 40$ GeV.

ACKNOWLEDGEMENTS

Alan Goodman (Tulane) and Glenn Beauvais (Simon Fraser University) were principal collaborators on the study of the liquid-gas phase transition question and their work on this problem is

happily acknowledged. This work is supported in part by the Natural Sciences and Engineering Research Council of Canada.

REFERENCES

1. Boal, D. H. and Goodman, A. L., Phys. Rev. C (in press).
2. Boal, D. H. and Shillcock, J. C., Phys. Rev. C33, 549 (1986).
3. Boal, D. H. and Reid, J. H., Phys. Rev. C29, 973 (1984).
4. See Finn, J. E., et al., Phys. Rev. Lett. 49, 1321 (1982) and references therein.
5. Bertsch, G., Kruse, H. and Das Gupta, S., Phys. Rev. C29, 673 (1984).
6. Gale, C. and Das Gupta, S., Phys. Lett (in press).
7. Beauvais, G. E. and Boal, D. H., University of Illinois report P/86/2/26.
8. A model which is formally equivalent to Ref. 7, although it differs in its application, has been advanced independently by Aichelin, J. and Stocker, H., Max Planck Institute (Heidelberg) report MPI H-1986-V6.
9. Boal, D. H. in Proceedings of the Workshop for Experiments for a Relativistic Heavy Ion Collider, Haustein, P. and Woody, G., eds., BNL Report and submitted to Phys. Rev.
10. Abramowicz, H., et al., Z. Phys. C17, 283 (1983).
11. Cutler, R. and Sivers, D., Phys. Rev. D17, 196 (1978).
12. Altarelli, G. and Parisi, G., Nucl. Phys. B126, 298 (1977).